

Data-driven Predictive Energy Optimization in a Wastewater Pumping Station

Jorge Filipe^{a,b}, Ricardo J. Bessa^{a,*}, Marisa Reis^a, Rita Alves^c, Pedro Póvoa^c

^a*INESC Technology and Science (INESC TEC), Campus da FEUP, Rua Dr. Roberto Frias, 4200-465 Porto Portugal*

^b*Faculty of Engineering, University of Porto, Rua Dr. Roberto Frias, 4200-465 Porto Portugal*

^c*Águas do Tejo Atlântico, S.A., Fábrica da Água, Av. de Ceuta, 1300-254 Lisboa*

Abstract

The wastewater management sector is being pushed to optimize processes in order to reduce energy consumption without compromising its quality standards. Energy costs can represent a significant share of the global operational costs (between 50% and 60%) in a energy intensive consumer. Recent advancements in smart water networks and internet-of-things technology create the conditions to apply data-driven optimization methods based on artificial intelligent techniques. Pumping is the largest consumer of electrical energy in wastewater treatment plant. Thus, the optimal control of pump units can help the utilities to decrease operational cost. This work describes a predictive control policy for wastewater variable-speed pumps that minimize electrical energy consumption, considering uncertainty forecasts for wastewater intake rate and information collected by sensors accessible through the SCADA system. The proposed control method combines statistical learning (regression and predictive models) and deep reinforcement learning. The results show a 16% decrease in electrical energy consumption while still achieving a 97% reduction in the number of alarms when compared with the current operating scenario.

Keywords: Reinforcement Learning, Predictive Control, Energy Efficiency, Data-driven, Machine Learning, Wastewater Treatment Plant

*Corresponding author

Email address: ricardo.j.bessa@inesctec.pt (Ricardo J. Bessa)

1. Introduction

1.1. Motivation

Drivers such as climate change, population, urbanization, aging infrastructure and electricity costs are all expected to impose significant strains on urban water cycle systems management. Water and wastewater management sector is confronted by the challenge of optimizing processes in order to reduce energy consumption and reduce the emission of greenhouse gases arising from water and wastewater transport and treatment without compromising water quality standards to which they are subjected [1]. It is important to highlight that energy costs represent a relevant component of water utilities operational costs and the water sector is an energy intensive consumer. For instance, the water sector represents 1.4% of the total electrical consumption in Portugal, including all the water and wastewater infrastructures (36% in wastewater infrastructures). In terms of total operational costs, energy consumption corresponds to around 57% (without considering human resources).

Additionally, the operational efficiency of wastewater services is generally lower, when compared to best practices in other industries [2], and it is expected that future quality standards become more restrictive and it will be necessary to improve existing treatments with the adoption of new technologies that may be intensive energy consumers. Recent advancements in smart water networks and internet-of-things are helping water and wastewater utilities to move in this direction, boosting efficiency and becoming more proactive in wastewater treatment [3].

Most of the processes that occurs in a wastewater treatment plant (WWTP) requires electrical energy for their operation and are intensive consumers. The pumping is the largest consumer of electrical energy in WWTP [4, 5]. Therefore, the control of pump units in WWTP can help the utilities to decrease operational cost (i.e., electricity cost) providing increased energy savings and environmental performance. The predictive control of pumping systems is the main objective of the present work.

1.2. Related Work and Contributions

Kalaiselvan et al. conducted a literature review of energy efficiency actions for pumping systems, grouped by component design, selection and dimensioning, control and

adjustment of variable-speed pump units [6]. The category “control and adjustment” was divided in the following sub-categories: (a) variable frequency drive control; (b) load shifting; (c) process optimization.

Load shifting has been an active area of research, mainly focused on the improvement the mathematical tractability and performance of non-linear and linearized (approximated) optimization models for scheduling the operation of pumping stations in water distribution systems, over a future period (e.g., day-ahead), to minimize electrical energy costs subject to constraints that account for the distribution system hydraulics [7, 8, 9]. Alternative approaches to the classical mathematical problems are meta-heuristics like evolutionary algorithms or genetic algorithms [10, 11] and model predictive control (MPC) approaches [12].

This problem is gaining new attention with demand-side management programs and opportunities created by the synergy between smart electric and water distribution networks [13]. This new paradigm requires tractable convex mixed-integer non-linear programming (MINLP) problems, robust to highly dynamic electricity tariffs [14], or the use of different variants of dynamic programming for solving the optimization problem [15]. Furthermore, opportunities like the participation in ancillary services (i.e., short term operational reserve, firm frequency response, frequency control by demand management) will emerge for flexible pumping systems [16].

All the aforementioned works share the following characteristics: i) are focused in operational scheduling of water distribution systems; ii) do not cover real-time control of pumping units (i.e., continuous optimization) and are designed for fixed-speed motored pumps (i.e., integer variables); iii) the formulations rely in approximations of the hydraulic model. Moreover, in WWTP, “long-term” flexibility (i.e., load shifting) is lower in comparison to water distribution. Therefore, most of the potential energy savings are a result of “short-term” flexibility, i.e., energy optimization close to real-time of variable-speed pumps. For instance, the MPC proposed by van Staden et al. in [12], can only be applicable in practice under certain conditions: i) constant or known water inflow rate; ii) large water reservoirs that allow pump scheduling in a 24 hours window (e.g., considering different electricity tariffs); iii) binary (on/off) control of pumps.

The present paper fits in the “process optimization” category and proposes an in-

novative data-driven energy optimization strategy of WWTP variable-speed pumps. It combines statistical learning (regression and predictive models) and artificial intelligence (AI) techniques. The main objective is to design predictive pump control policies that minimize electrical energy consumption, considering uncertainty forecasts for wastewater intake and information collected by sensors that are typically installed in WWTP and accessible through the SCADA system. Constraints related to the desired output (i.e., wastewater output flow, head) are also included. Furthermore, this control approach does not require an explicit (or mathematical) model of the process since the system dynamics are learned from the data.

For this problem, the industry state of the art is to turn on/off pumps according to a level-based control system. For instance, this patent [17] describes a method for operating a pumping system of a WWTP where the pump starts operating if a level of a wastewater in a tank exceeds a first level, and the pump stops pumping if the level of the wastewater in the tank drops below a second level. However, control algorithms based on soft computing are earning attention and being explored for WWTP and water distribution systems, mainly in cases where the physical (or mathematical) model is not available or is too complex to be integrated in a classical controller.

Fiter et al. described a fuzzy logic controller to regulate the aeration in the bioreactor of a WWTP [18]. The controller integrated information from two signals, dissolved oxygen and oxidation-reduction potential values, to minimize the electrical energy consumption. Reinforcement learning (RL) was also applied to optimize different processes in WWTP. Syafie et al. proposed a model-free control approach for advanced oxidation processes (or Fenton process) since according to the authors it is extremely difficult to develop a precise mathematical model and the system is subjected to several uncertainties and time-evolving characteristics [19]. As an alternative to proportional–integral–derivative (PID) controllers, Hernández-del-Olmo et al. explored RL for oxygen control in the N-ammonia removal process, which main objective was to minimize WWTP operational cost (including energy costs) [20]. Asadi et al. optimized water quality and energy consumption of the aeration process by combining boosting trees for feature selection and different machine learning algorithms (e.g., artificial neural networks, random forests) for modeling the relationship between input, controllable and output variables [21].

More related with the work of the present paper, Kebir et al. described a rule-based method to control WWTP pumps according to the measured wastewater tank level and minimize electrical energy consumption by using a fuzzy logic controller that work as follows: on rainy day's pumps react faster and frequency is increased quickly to avoid flooding; on dry day's pumps can react more slowly and frequency is decreased softly to prevent draining of the tank [5].

Data mining algorithms were also explored to optimize the pump operation, including the modeling of input and output variables. Wei and Kusiak applied static multi-layer perceptron and dynamic neural networks to forecast the influent flow in WWTP [22]. Zhang and Kusiak tested seven data mining algorithms based in 5-min and 30-min data to construct a pump energy consumption model and a water flow rate (after the pumps) model of the preliminary treatment process of a WWTP [23]. These two data-driven models were incorporated in different formulations of an optimization problem to generate optimal pump schedules: (a) MINLP problem to reduce energy consumption solved with particle swarm optimization [24] or with greedy electromagnetism-like algorithm [25]; (b) bi-objective optimization solved with artificial immune network algorithm to minimize the energy consumption and maximize the pumped wastewater flow rate [26]. These optimization models can be enhanced with a discrete-state Markov process for modeling the maintenance decisions [27].

Considering the revised literature, the present paper produces the following original contributions. Applies a model-free and data-driven control approach based in RL, in contrast to the use of meta-heuristics [24, 25, 26] or fuzzy logic control [5]. The control philosophy is focused in operating the tank with a variable water level, instead of controlling the frequency increase/decrease rate like in [5]. The vector of system states from RL is modified to include probabilistic forecasts of wastewater intake and implement a predictive control of the pumping system, which was never proposed in the literature. Finally, a real-world implementation of the RL control method is made possible by applying data-mining algorithms to construct models from data and generate synthetic data for pre-training the RL algorithm, without the need to physically interact with the system. This also represents an original contribution compared to other control problems like [20, 19].

Finally, the proposed method is applied to a real case-study and avoids the use of simplifications or simulation models for the physical system.

1.3. Structure of the Paper

The remaining of the paper is organized as follows: section 2 describes the wastewater treatment process and a real-world pumping station; section 3 presents the data-driven control framework and its different modules; section 4 describes the probabilistic forecasting method for the wastewater intake rate time series; section 5 presents the environment emulation method and predictive control method; the numerical results are discussed in section 6 and main conclusions provided in section 7.

2. Wastewater Treatment Process Overview

A wastewater treatment system is composed by a drainage system, a WWTP and the discharge infrastructure. Traditionally, a WWTP is divided into mechanical, physical, chemical and biological treatment, which has been utilized with many different combinations and organized in different treatment phases [28]: pre-treatment, primary treatment, secondary treatment (biological), tertiary treatment, disinfection, sludge treatment and odor control.

This work is focused in the control of wastewater pumping stations in a WWTP, Fábrica da Água de Alcântara, Portugal. The case-study corresponds to the wastewater pumping station (WWPS) between primary and secondary treatment, as depicted in Figure 1, which is composed by five pump units of 110 kW each.

The primary treatment involves the separation of macrobiotic solid matter from the wastewater using primary clarifiers. This solid matter is later pumped out of the tanks for further treatment and the remaining water is then carry out for secondary treatment. Secondary treatment is applied to degrade the biological content of the sewage that are derived from human waste, food waste, soaps and detergent.

The current pump control policy of the WWPS consists in operating at fixed water level (6 meters) and turning on/off the pumps when the measured level is below/above the predefined value. The water intake is not controllable and the output wastewater for

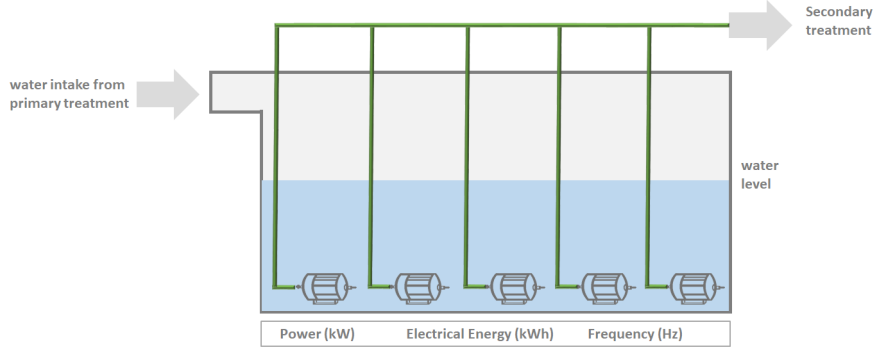


Figure 1: Wastewater pumping station with 5 units of 110 kW.

the secondary treatment is controlled by the pumping unit's operation. The constraints for the wastewater level are a minimum of 3 meters and a maximum of 8 meters.

It is important to stress that this case-study consists of a single pumping station, but the wastewater treatment system has a total of 13 analogous processes, and the company a total of 292 stations. Therefore, in order to replicate the proposed control policy it is only necessary to have variable-speed pump units and the variable collected by the SCADA system (see next section).

3. Data-driven Predictive Control Framework

3.1. General Control Philosophy

The proposed data-driven control framework aims at optimizing the energy consumption of WWPS by optimally defining the operating set point for each variable-speed pump unit. Given the layout of the WWPS, described in section 2, electrical energy gains can be achieved by operating with a higher wastewater level, in order to reduce the relative height between the wastewater level and the secondary treatment tank. However, operating with a higher level also increases the risk of wastewater overflow, due to the uncontrollable and volatile rate of the wastewater intake from the primary treatment.

Presently, the wastewater pumping stations are operated with fixed-level control rules. This sub-optimal solution has the same buffer (difference between the maximum height of the tank and the threshold) independently of the season. In dry seasons there is a lower wastewater intake rate (WWIR), therefore the station could be operated with a

higher level without impacting the safety of the operation. On the other hand, during wet seasons, which have a much higher and volatile WWIR, could, dynamically, reduce the wastewater level to accommodate extreme WWIR.

The proposed predictive control has the ability to anticipate the incoming WWIR and to adjust the reservoir buffer accordingly. For this, the algorithm relies in two main functions: i) WWIR forecasting and ii) AI control based on RL.

Probabilistic forecasts of the WWIR are generated and used as one of the inputs of the AI control algorithm, in order to provide not only a set of quantiles indicating the WWIR but also providing the control strategy with information about forecast uncertainty.

The AI control relies on RL concepts. RL is a machine learning method which contrasts heavily with more traditional AI classes, such as supervised learning (SL). In SL, the fitting of a model is made through instructive feedback, so there is a tangible path to improve the model (loss function). In RL, the learning process is made by evaluative feedback, which translates in knowing how well you achieved your goal (reward). For each learning instant, the RL algorithm uses as input a set of variables that are able to provide a snapshot of the environment and these values are used to sample an action. This action will result in a state transition that will produce a reward. Through several interactions with an environment, the control policy will learn the optimal action or course of actions that maximize the expected reward. Figure 2 illustrates the learning process adapted for the case study of this work. The state is described as a set of variables characterizing the WWPS, e.g. tank level, wastewater intake rate forecasts, pumps available and its current operational set-point, etc. Actions extracted from the control policy are the set-point for each pump unit. The reward that provides feedback on the performance of the model is the pumps' electrical energy consumption.

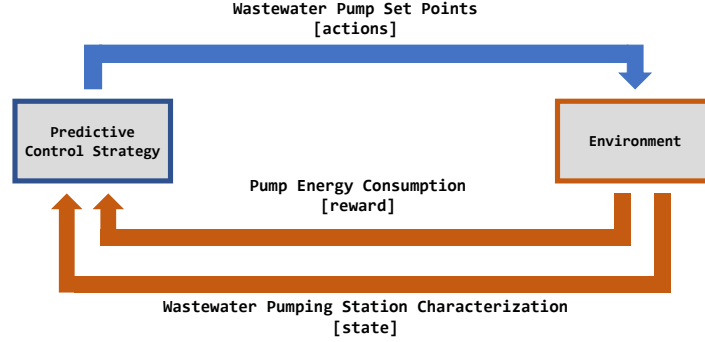


Figure 2: Reinforcement Learning applied to wastewater pumping station.

When dealing with physical systems composed by expensive mechanical components and in continuous operation, it is impossible to directly implement a control algorithm that relies on thousands of interactions with the system to learn the optimal control policy. Therefore, a two-stage framework was developed: i) initial learning and ii) operational stage.

3.2. Initial Learning Stage

This first stage is responsible for conducting an initial learning of the control policy. Historical data is collected from the SCADA system of the WWPS, containing information about the pumps (active power and frequency) and the wastewater tank (reservoir level, WWIR and outflow rate). This data is used in three modules: WWIR forecasting, episodes creation and environment emulation, as depicted in Figure 3.

- The forecasting module uses the historical time series of WWIR in order to produce probabilistic forecasts, as will be described section 4.
- The WWPS operation is continuous. However, in order to maximize the historical information used to train the control algorithm, the complete time series was divided into a set of episodes with unequal length. Each step represents 2-minute discrete interval of the WWPS and has the following information: pumps online, current pump set-point, WWIR, original wastewater level and WWIR forecast for 20 steps ahead (40 minutes). At the start of each episode, the initial water level is randomized in order to increase the diversity of the learning dataset. These

episodes are then sampled randomly and used in the learning process of the RL control.

- The environment emulation module applies statistical learning algorithms to the historical data in order to emulate the physical processes: i) relation between pumping power and outflow rate and ii) modeling of the reservoir level deviation as a function of the WWIR and outflow rates. Both methods are detailed in section 5.1.

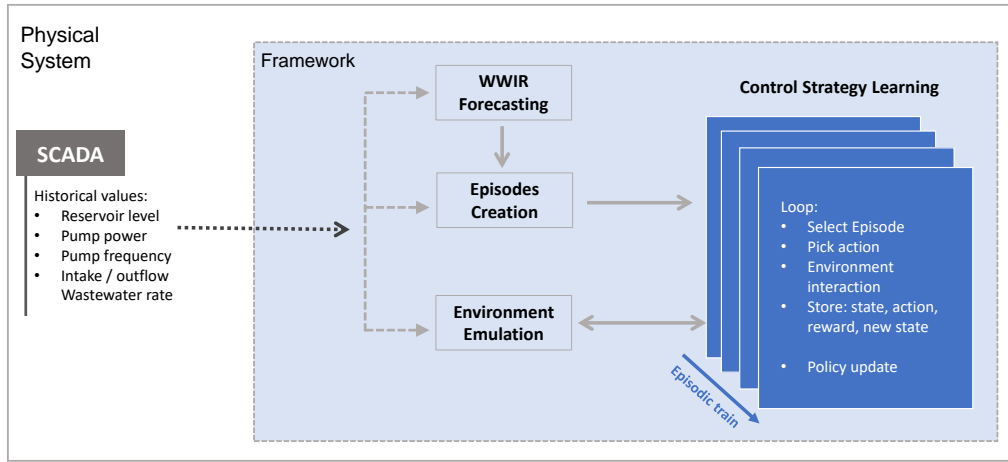


Figure 3: Initial learning stage of the data-driven control method.

To summarize, from the historical data collected via SCADA system the following information is created: i) WWIR probabilistic forecasts; ii) data-driven models that emulate the physical environment; iii) episodes combining historical data and forecasts.

The learning process uses this information in the following way:

1. Select an episode
2. Randomize the initial water level
3. For each step of the episode:
 - (a) Collect the state characterization
 - (b) Sample an action from the control policy
 - (c) Apply the action to the emulated environment
 - (d) Observe the state transition

- (e) Collect the reward
 - (f) Store the vector [state, action, reward, new state]
4. Update the control policy (according to section 5.2)

After thousands of episodes, the control policy will learn which action (or set of actions), for a given state, results in the higher expected reward in the long term.

3.3. Operational Stage

After the initial learning stage, the control policy is optimized and ready to be integrated with the physical system. However, due to inconsistencies between the emulated and physical system, some interactions with the real environment are necessary to calibrate the policy.

During the operational stage, the overall process, as depicted in Figure 4, is the following:

1. Collect the state characterization from the SCADA
2. Generate the WWIR probabilistic forecasts
3. Sample an action from the control policy
4. Apply the action to the physical environment
5. Observe the state transition
6. Measure the power consumption (reward)
7. Store the vector [state, action, reward, new state]
8. Update the control policy (according to Section 5.2)

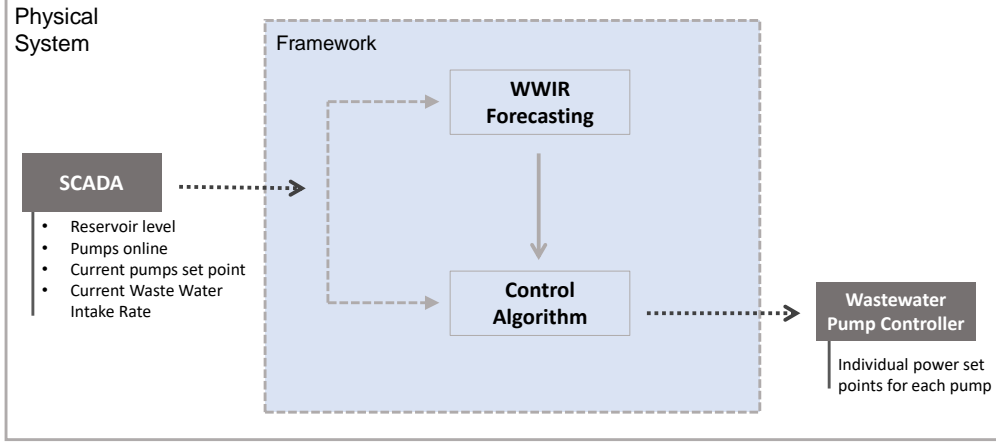


Figure 4: Operational stage of the data-driven control framework.

4. Forecasting Wastewater Intake

This section describes a multi-step ahead forecasting method for the WWIR, considering both point (i.e., expected value) and probabilistic representations. This requires the use of statistical learning algorithms, as well as the creation of additional features from the raw dataset (i.e. feature engineering) and select a subset of explanatory variables.

4.1. Feature Engineering

An important characteristic of the time series and with impact in the feature creation is that measurements are collected with irregular sampling frequency. About 68.9% of the observations are sampled with 2 minutes interval, followed by 3 minutes sampling with 16.1%, and 8.5% of observations above 5 minutes. Figure 5 depicts three sample periods of the WWIR time series, where it is possible to observe the irregular sampling of the time series.

This is particularly challenging for including lagged variables (i.e., past values of the time series) in the forecasting model, according to an autoregressive framework. To overcome this limitation and enable the inclusion of lagged variables, a re-sampling is performed over an uniform time interval. In this case, it was re-sampled to the most common observed time frequency, which was 2 minutes.

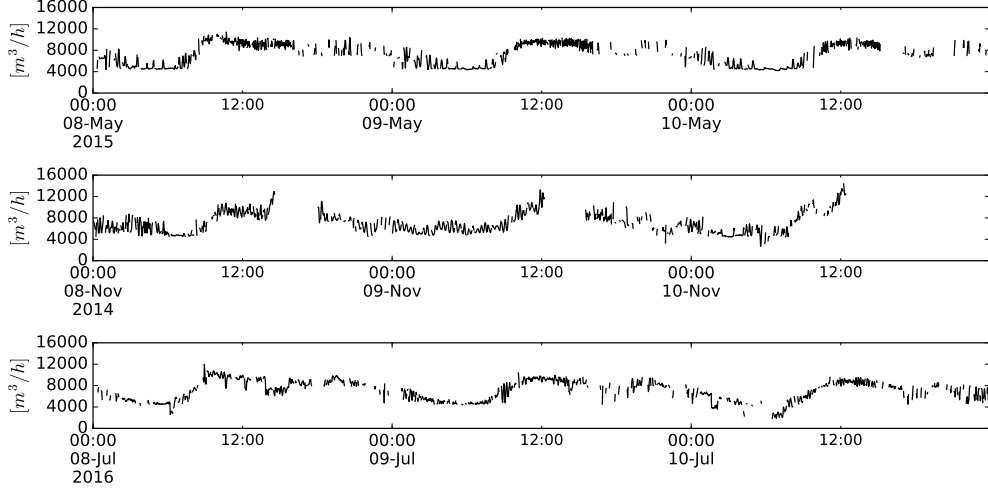


Figure 5: WWIR time series sample period (May, November and July).

Figure 6 depicts the autocorrelation function computed over the re-sampled time series. The plot provides the correlation as a function of the lags when comparing the original series with the lagged version of itself. As we can observe, the time series exhibits significant serial correlation with smaller lags, and a peak is observed around $lag = 720$. The latter indicates a daily seasonality, since $lag = 720$ with 2 minutes resolution corresponds to the previous day. Based on this information, lagged features were added to the model, W_{t-1}, \dots, W_{t-l} where l is the number of lags to be determined, as well as the WWIR from the same timestamp of the previous day, denoted as $^{24H}W_t$.

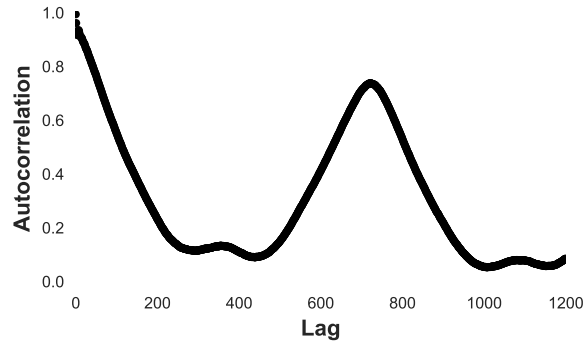


Figure 6: Autocorrelation function plot for the WWIR time series.

The average WWIR strongly depends from the period of the year and period of day, as depicted in the boxplots of Figure 7. From the hourly pattern, it is possible to observe higher variability in the period between 7:00 and 9:00, with change of the average and quantiles daily curve. For the monthly analysis, higher values are observed in for winter months. January and February in 2014 show an average 9816 m^3/h and 10832 m^3/h intake respectively. The monthly variation is mainly due to the higher precipitation levels. In November 2014, higher distribution with 10076 m^3/h mean WWIR are also observed. This analysis suggests that calendar variables, like the hour of the day, month and weekday should be included the forecasting model.

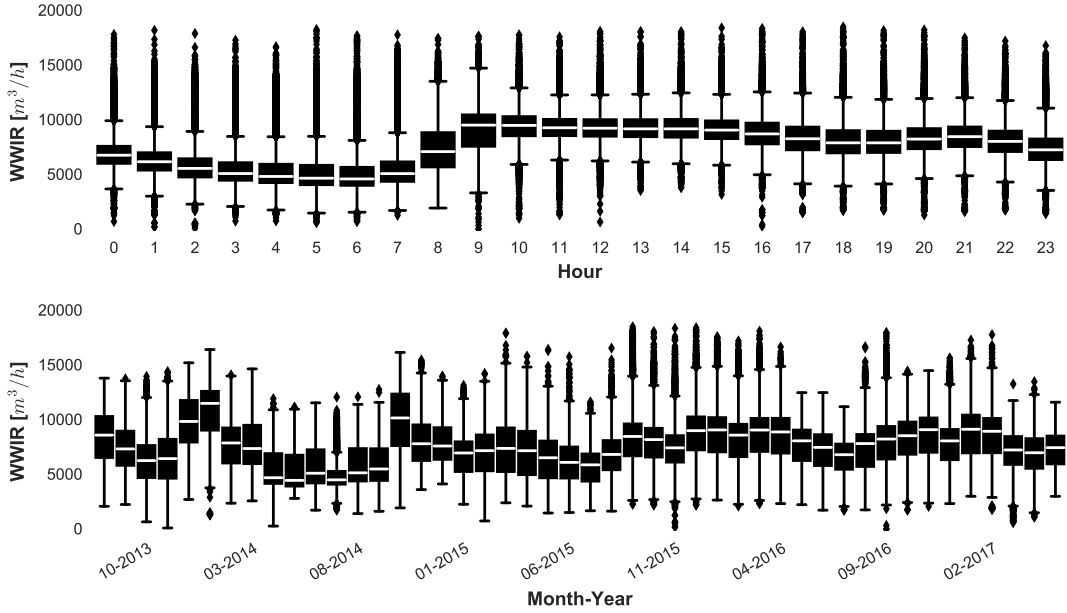


Figure 7: Hour and monthly boxplots of WWIR.

In addition to the classical lagged and calendar variables, from the raw variables dataset it is possible to derive additional features. Considering the WWIR time series represented by $W = \{W_1, \dots, W_n\}$ and its timestamp represented by $\{t_1, \dots, t_n\}$, the following new features were calculated as follows:

- Change over Time (CoT): $c_m = (W_{m-1} - W_m) / (t_{m-1} - t_m)$
- Growth or Decay (GoD): $(W_{m-1} - W_m) / W_m$

In summary, the features considered for the forecasting model are: i) calendar variables such as hour, weekday and month; ii) lagged variables close to launch time t $-W_{t-1}, \dots, W_{t-l}$ and 24 hour lag $-^{24H}W_t$, iii) difference series translating change $-CoT_{t-1}$ and slope growth or decay $-GoD_{t-1}$. Note that except for the calendar variables, all the features are build backward-looking, in the sense that each point of the time series only depend on past values.

4.2. Forecasting Model

The objective of the forecasting model is to obtain a model that approximates an unknown regression function $W = f(\mathbf{x})$, where \mathbf{x} is the set of features described in the previous section. In order to produce multi-step ahead forecasts, a model is fitted for each lead-time $t + k$ as follows:

$$\begin{aligned}\hat{q}_{t+1} &= f_1(W_{t-1}, \dots, W_{t-l}, \text{hour}, \text{wday}, \text{month}, CoT_{t-1}, GoD_{t-1}, ^{24H}W_{t+1}) \\ \hat{q}_{t+2} &= f_1(W_{t-1}, \dots, W_{t-l}, \text{hour}, \text{wday}, \text{month}, CoT_{t-1}, GoD_{t-1}, ^{24H}W_{t+2}) \\ &\vdots \\ \hat{q}_{t+k} &= f_k(W_{t-1}, \dots, W_{t-l}, \text{hour}, \text{wday}, \text{month}, CoT_{t-1}, GoD_{t-1}, ^{24H}W_{t+k})\end{aligned}\tag{1}$$

where l is the number of lags, $t + k$ is the lead-time horizon and $\hat{q}_{t+k} \equiv \hat{q}_{t+k}^{(\alpha_i)}$ denotes the forecast for the quantile with nominal proportion α_i issued at time t for forecast time $t + k$. In order to produce these forecasts, f is fitted for each step ahead with information available at time t for the k horizons.

In this work, two different statistical learning algorithms were considered for modeling function f :

- Linear Quantile Regression (LQR) [29], which is a linear model analogous to multi-linear regression but with the possibility to adjust a specific model to generate a conditional quantile estimation. This model is available in the STATSMODELS library[30].
- Gradient Boosting Tress (GBT) [31], which is an ensemble of regression trees as base learners and presents a high flexibility in accepting different types of loss functions. In this work, the quantile loss function is used to generate probabilistic forecasts. The model is available in the SCIKIT-LEARN library [32].

4.3. Forecasting Skill Metrics

The forecasting skill of the wastewater inflow was evaluated for both point and probabilistic forecast. The quality of the probabilistic forecast was access with the following metrics: calibration, sharpness and continuous rank probability score (CRPS). A completed description of these metrics is given in [33, 34], and the following paragraphs present a general description of these metrics.

Calibration measures the deviation between empirical probabilities (or long-run quantile proportions) and nominal probabilities. This difference is also called bias of the probabilistic forecasts and is usually calculated for each quantile nominal proportion (τ). Sharpness quantifies the degree of uncertainty in probabilistic forecasts, which numerically corresponds to compute the average interval size between two symmetric quantiles (e.g., 10% and 90% with coverage rate γ equal to 20 %).

CRPS is an unique skill score that provides the entire amount of information about a given method's performance and encompasses information about calibration and sharpness of probabilistic forecasts. The CRPS metric was adapted to evaluate quantile forecasts, as described in [34]).

Point forecasts, i.e. 50% quantile in this work, were evaluated with the classical Mean Absolute Error (MAE).

4.4. Forecasting Skill Results

4.4.1. Benchmark Models

Typically used in the literature, the persistence model assumes that the forecast for $t + 1$ is equal to the value observed in the previous time step t . Due to the strong correlation between time instants t and $t - 1$, a naive algorithm such as this one can be very hard to beat in terms of forecasting performance, especially for very-short time horizons and in dry periods with low variability.

In addition to persistence, LQR model conditioned to the period of the day (i.e., hour) is also considered as a second benchmarking model. With this benchmark method, we allow the distribution to change for each period of day. This method will be denoted *CondbbyHour*.

4.4.2. Variables Importance

This subsection evaluates whether or not the input features improve the forecasting skill, measured with the MAE and CRPS. This evaluation is performed only for the first lead time ($t + 1$) using the LQR. The choice on the number lags was made by calculating the MAE of different models having different numbers of lags as explanatory variables (parameter l), using a out-of-sample period. Figure 8 depicts the MAE as a function of the number of lags, and it is possible to see that MAE stops decreasing after $l = 8$. Therefore, variables W_{t-1}, \dots, W_{t-8} are included in the final model.

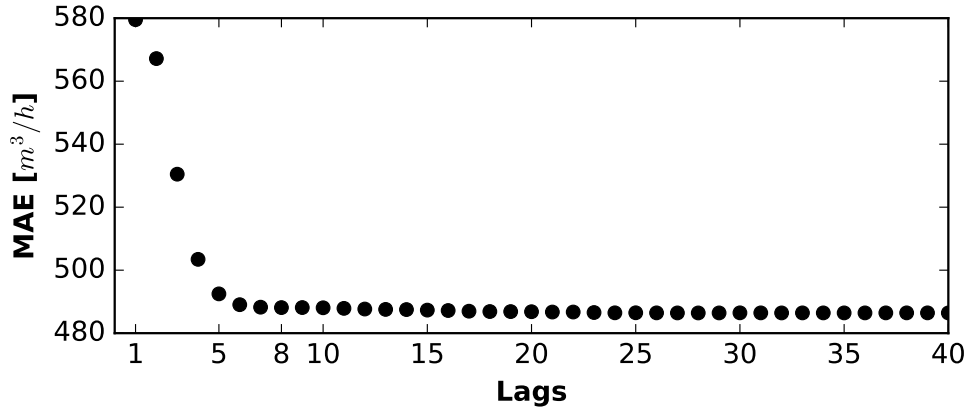


Figure 8: MAE as a function of the number of lags.

Additionally, the improvement obtained by including variables CoT , GoD , and ^{24H}W was quantified. Table 1 summarizes the feature selection results. Each row is a model, and each cell in the row is filled if the corresponding column (variable) is included in the model. The last two columns are the forecast performance obtained with the corresponding model. The performance metrics are negatively oriented, meaning small values are better.

Table 1: Forecasting skill for different combination of features.

Model	Calendar			Lags	$^{24H}W_{5,t}$	CoT	GorD	Evaluation Metrics	
	hour	wday	month					MAE	CRPS
M1	x							1428	1382
M2					x			1077	1096
M3				x				487	640
M4	x	x	x					1153	1109
M5	x	x	x			x		1118	1087
M6	x	x	x				x	1117	1086
M7	x	x	x	x	x			472	621
M8	x	x	x	x	x	x		356	538
M9	x	x	x	x	x		x	361	542
M10	x	x	x	x	x	x	x	353	535

The model conditioned to the hour of the day (M1) shows the worst performance with $1428 \text{ m}^3/h$ of MAE. Adding the other calendar variables (M4), the error is improved with respect to M1. But, when considering only the combination of calendar variables (M4) and *CoT* or *GorD* variable (M5 and M6), these models do not offer competitive performance in comparison with the inclusion of lagged information (M2 and M3). This is clearer with model M3. The combination of Lags ($t - 1 \dots t - 8$) and measurement from the previous day, results in a minor decrease of both metrics (model M7). Having *CoT* or *GorD* with lagged variables (M8 and M9) show similar errors $CRPS = 356 \text{ m}^3/h$ and $CRPS = 361 \text{ m}^3/h$ respectively. But, when both are added in M10, a further error reduction is attained with $CRPS = 353 \text{ m}^3/h$. The best model is achieved with all the features (M10). In overall, the inclusion of the lagged variables provides the largest error reduction. In conclusion, all features constructed in section 4.1 are considered relevant and included in the final model.

For completeness, we include here the analysis obtained with the GBT model since it can automatically provide estimates of feature importance from the in-sample dataset. The feature importance is calculated explicitly for each variable in the dataset, allowing variables to be ranked and compared to each other. The importance is given in a percentage score that indicates how useful or valuable each feature was in the construction of the decision trees within the gradient boosting model. Figure 9 illustrates the feature

importance given by the GBT model for lead-times between $t+1$ and $t+20$. The features with higher score are W_{t-1} and the hour of the day. We can observe that when the time horizon increases, the importance of features based on recent lags decrease compared to calendar variables. This more notorious in the case of the *wday* feature, since in the first lead time the importance score is almost null.

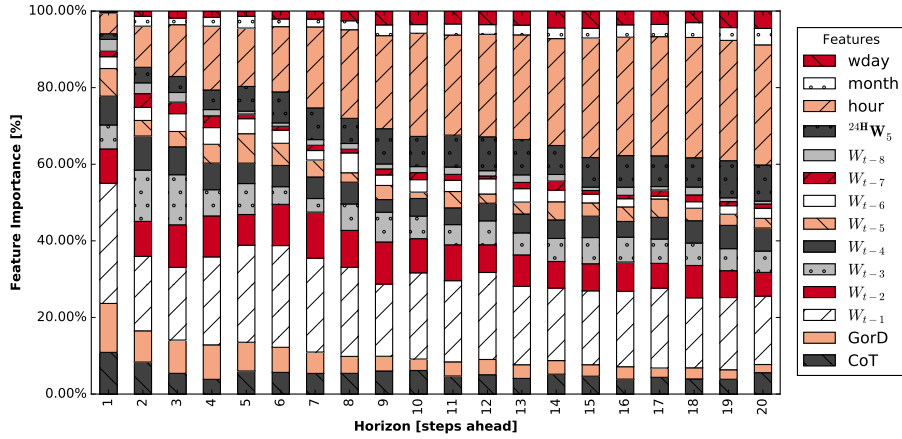


Figure 9: Feature importance determined by the GBT model.

4.4.3. Performance Evaluation

The WWIR dataset comprises 470,962 observations from the period between September 2013 and June 2017 with non constant sampling frequency. After the resampling to the 2 minutes time interval, the resulting dataset comprised 460,896 observations.

The forecasting skill was evaluated by splitting the intake dataset into an in-sample period, used for the initial parameter estimation and model selection, and an out-of-sample period, used to evaluate forecasting performance.

The hyperparameters optimization was performed using Bayesian optimization [35] with 3-fold as cross validation on the in-sample period. Results are obtained for the out-of-sample sample period.

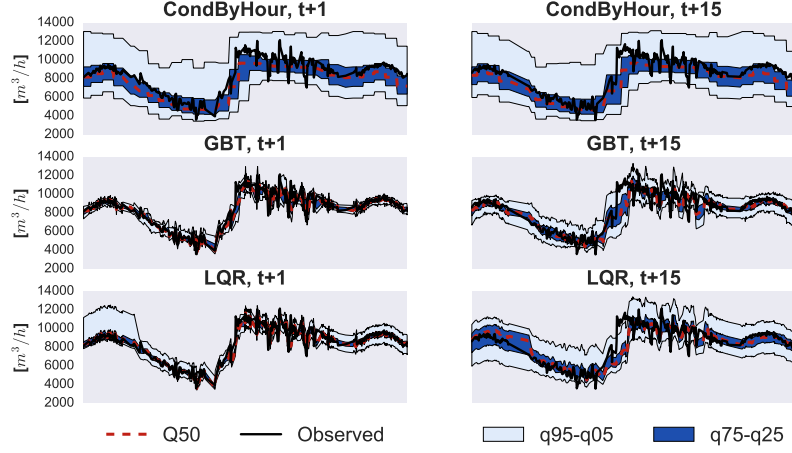


Figure 10: Probabilistic forecast example for horizons 1 and 15 steps ahead. The blue regions show 50% and 90% prediction intervals. In black solid line the observed WWIR.

Figure 10 present an example of probabilistic forecast for lead-times $t + 1$ and $t + 15$, obtained with CondByHour, LQR and GBT models. The linear model with the hour as single variable (CondByHour) exhibits low sharpness (wide predict intervals), as the model does not condition to recent WWIR values. As expected for larger horizons the uncertainty grows, for the first horizon both LQR and GBT provide (narrowed predicted intervals) when compared with the forecast for the 15 steps ahead.

The forecasting skill results are presented in Figure 11 for all metrics. The left-top plot depicts the difference from the “perfect calibration” (i.e., perfect match between nominal and empirical probabilities represented by the red line) averaged across all time horizons. The *CondByHour* model showed the worst calibration of the three models, underestimating the forecast (negative deviation from perfect calibration). The remain quantile models (GBT and LQR) underestimate quantiles bellow 50% and overestimate up to quantile 50%. In terms of calibration GBT presents the best performance, being the deviation from the ideal (red line) smaller along all nominal quantile probabilities. Nevertheless, in all cases the deviation is within the interval -3% and 3%.

Concerning sharpness (left bottom plot), the goal is to have small amplitude of forecast intervals for all coverages rates. Again, *CondByHour* showed forecast intervals with wider amplitude, average interval size varying from 327 to 6075 m^3/h for increas-

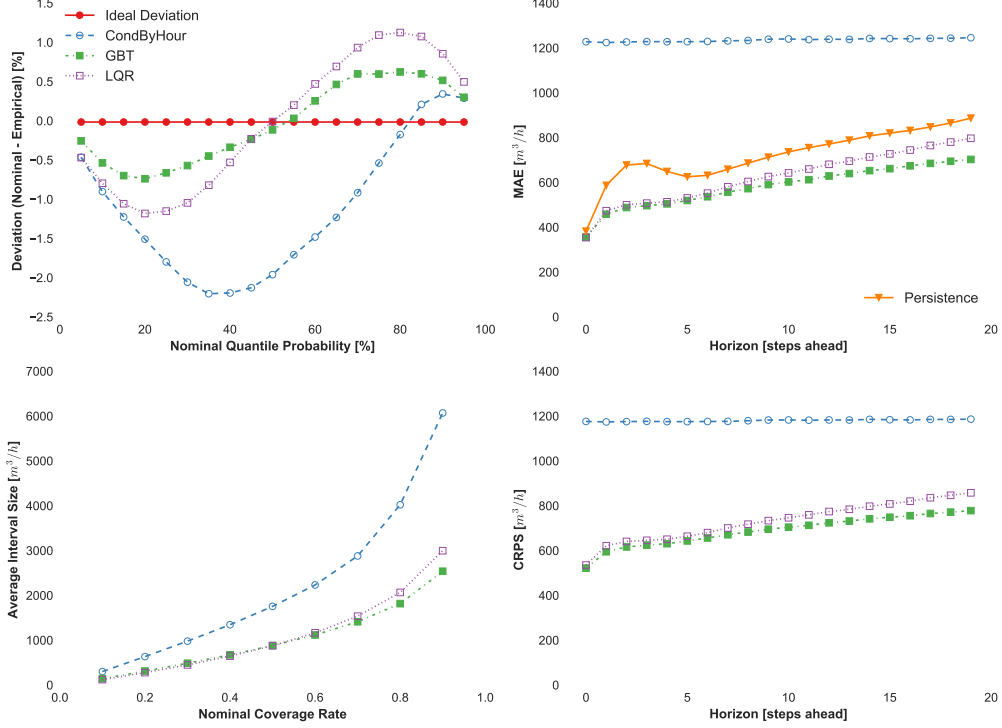


Figure 11: Forecasting skill results for point and probabilistic forecasting.

ing nominal coverage. *LQR* and *GBT* for the same nominal coverages showed much sharper intervals (almost half of the amplitude). Also in Figure 11, the MAE and CRPS results are given for each step ahead and with the same units of the wastewater inflow m^3/h . We can see that *CondbyHour* has the worst performance, with constant errors $MAE=1240m^3/h$ and $CRPS=1185m^3$ spread across the forecast horizon. Persistence results are only present for this metric, since it corresponds to point forecasts. As observed, persistence offers a very competitive forecasting skill. The GBT model (in green) presents the best performance in both metrics, following LQR in second place. The probabilistic forecasts from this model are used in predictive control strategy of the following sections.

5. Process Modeling and Predictive Control

5.1. Environment Emulation Model

As mentioned before, the RL methods require thousands of interactions with the environment in order to find the action or course of actions that maximize the expected reward. Since it is impractical, from an implementation point of view, to learn and interact from scratch directly with the physical system, it is necessary to emulate the environment. This emulation relies in the two modules described in sections 5.1.1 (wastewater outflow rate) and 5.1.2 (wastewater level of the tank).

Figure 12 depicts the interaction, for each episode, between the control policy and emulated environment.

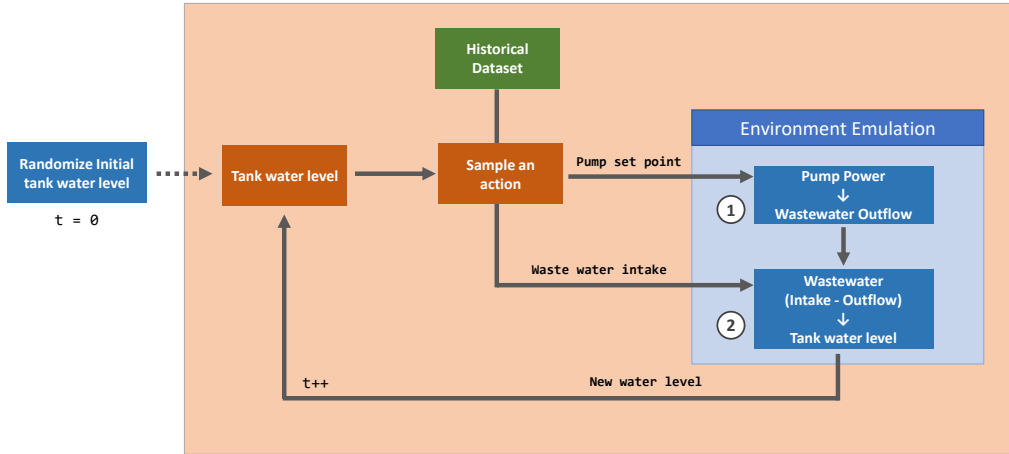


Figure 12: Episodic training of the control policy.

At the start of the episode, the initial wastewater level of the tank is randomized, while for the following steps the water level is a result of the actions defined by the control policy. The following processes occur cyclically until the maximum number of steps in the episode is reached. An action is sampled from the stochastic control policy that comprises the individual operating set-point of all the pumps and applies them to the emulated environment. The first model uses this information to obtain the resulted wastewater outflow rate, which combined with WWIR (gathered from the historical dataset) allows the second one to model the tank wastewater level for the next instant.

This new value is used at the start of the loop as the actual wastewater level and the cycle is repeated.

The following sections present details of the two models used to emulate the physical system, which are based in statistical learning algorithms.

5.1.1. Modeling Wastewater Outflow Rate

Knowing the operational set-point of each individual pump (selected by the control policy) and the current level of wastewater of the tank, it is possible to estimate the amount of wastewater that will be pumped from the tank. The statistical learning algorithm GBT was used to model this relationship between pump power and wastewater outflow. For this model the following input features were used:

- Individual pump power set-point [float - kW]
- Active pumps [binary]
- Number of pumps active [integer]
- Total power consumption [float - kW]
- Tank water level [float - meters]

The data-driven approach allow us to model the pumping station environment simply by using historical data. However, this particular dataset contained some inconsistencies due to noisy readings, but also due to a safety mechanism implemented in the pumping station. When the water level is above 7.2 meters a portion of the wastewater is routed to the output of the wastewater, skipping some treatment stages. However, the SCADA system continues to collect data during these instants, leading to incorrect records. The first issue was minimized by applying a re-sampling technique which decreases the time resolution of the dataset from an average of 2 minutes for each reading to 4 minutes, reducing the number of samples but smoothing the records. For the second issue, all records registered when the wastewater level was above 7.2 meters were excluded from the learning dataset of this model.

Trying to optimize every hyper-parameter of the GBT model would allow us to improve the model's performance in the learning dataset, which typically is a good approach for a regression problem (note that we are not making forecasts). However, in a dataset with noise and incoherent readings, it would result in a model that does not accurately represent the actual physical system. Furthermore, as illustrated by Figure 13, if the

RL algorithm discovers an operational range like the ones shaded, it will exploit this zone over and over leading to a different performance when moving from the simulation environment to the operational deployment.

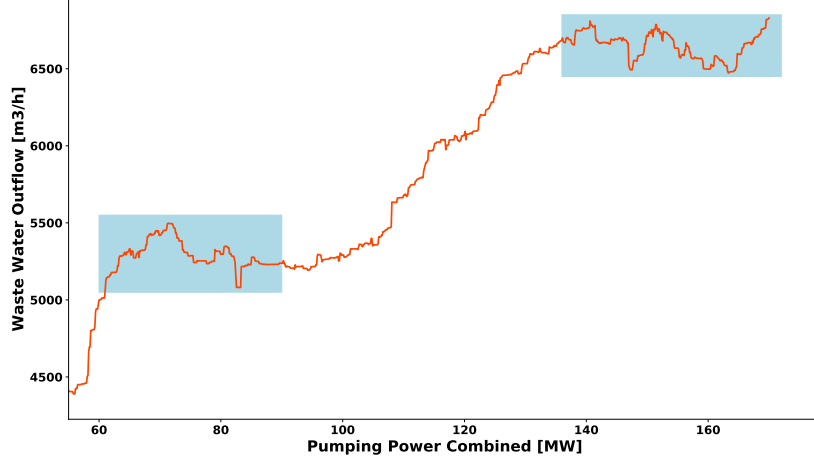


Figure 13: Overfitted pump power to wastewater outflow model.

The analysis of typical wastewater pumping curves allowed to conclude that the relationship between power, outflow and tank level is represented, typically, by a monotonic increasing curve, in contrast with the curve displayed in Figure 13, which shows neither one of these characteristics. The integration of this domain knowledge into the data-driven approach has the potential to achieve a better modeling of the pumping station, and can be achieved by tweaking the hyper-parameters of the GBT training process. Decreasing the maximum depth of the individual regression estimators, limiting the number of nodes in the gradient boost tree, forces the model to generalize better and avoids the excessive overfitting to the training dataset. Despite achieving a lower error metric when applied to the historical dataset, the model is able to better represent the physical system and, therefore, it is easier to be moved from simulation to physical application (requiring just a few interactions with the physical environment to calibrate the RL agent).

Figure 14 depicts, in four different operating scenarios, the results of the fitted model in which it is possible to observe the amount of wastewater outflow as a function of the total power consumption and the current level of the tank. One can verify the impact of the tank level in the efficiency of the pumps, i.e. higher the level, lower is the required

power consumption. It is also possible to observe that the new GBT model outputs pumping curves with monotonic and increasing behavior.

The GBT model showed a MAE of $350 \text{ m}^3/\text{h}$ and a root mean squared error (RMSE) of $478 \text{ m}^3/\text{h}$ in an out-of-sample dataset.

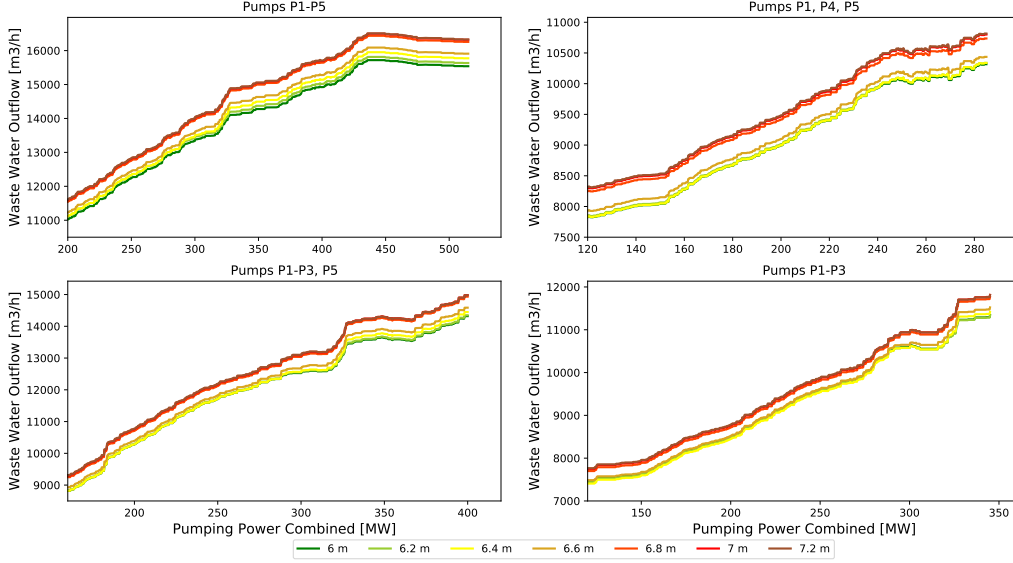


Figure 14: Examples of the pump power to WW outflow model for different water levels.

5.1.2. Modeling Reservoir Wastewater Level

With information about the amount of WWIR entering the tank (by acquiring sensor data from the SCADA system) and knowing the amount of wastewater being pumped as result of the pumps operation (from the previous model - section 5.1.1), it is possible to model the change in the tank level.

Given the physical characteristics of the tank, this relationship can be modeled using a multi-linear regression model. The features used as input were: current wastewater tank level, WWIR, wastewater outflow rate and the difference between the intake and outflow. Using the linear regression method from the Python SCIKIT-LEARN library [32] the model achieved a MAE of 4.32 centimeters and a RMSE of 6.74 centimeters.

5.2. Control Policies

The control policy relies on RL to optimize the operation of the WWPS. A standard RL setup consists of an agent interacting with an environment E in discrete timesteps. At each timestep, the agent receives an observation s_t (characterization of the state), takes an action a_t and receives a scalar reward $r_t(s_t, a_t)$.

The agent behavior is defined by a policy $\pi_\theta(a|s_t)$ which samples an action given the current state and the policy parameters θ . The aim of the agent is to maximize the sum of expected future rewards discounted by γ : $\mathbb{E}_\pi[R_t] = \mathbb{E}[\sum_{i \geq 0} \gamma^i r(s_{t+i}, a_{t+i})]$.

5.2.1. Agent

The RL algorithm used to train the control policy is the Proximal Policy Optimization (PPO) [36]. PPO is a policy gradient method, which alternates between sampling data through interaction with the environment and optimizing a surrogate objective function using stochastic gradient ascent.

The above mentioned PPO algorithm, typically, uses an advantage estimator based on the Generalized Advantage Estimation (GAE) [37], as described in Equation 2, where $V(s_t)$ is the estimated value at the state s and instant t , and γ is the discount factor. To calculate this advantage it is necessary to collect experiences for T time steps and calculate the discounted advantage for all these time steps, so with $T = 200$ the advantage at the first time step will be composed by all the discounted rewards until the last time step. This can lead to volatile results due to the credit assignment problem. In this work, we used a truncated GAE, so only a small part of all the experiences receive the discounted advantage, in order to better account the characteristics of the state vector. Since the WWIR forecasts used have a lead time of 20 steps ahead, it makes sense to limit the discounted advantage to the same interval, i.e. $T = 20$.

$$\hat{A}_t = -V(s_t) + r_t + \gamma r_{t+1} + \dots + \gamma^{T-t+1} r_{T-1} + \gamma^{T-1} V(s_T) \quad (2)$$

The policy trained by PPO is represented by a neural network (NN) with two layers of 64 neurons and using the rectified linear unit as the activation function. The NN receives as input the state vector and outputs the parameters of a probability density function. Since the actions selected by the RL agent are within 0 and 1, corresponding

to the set-point of each pump unit, a multivariate Beta distribution was used. Therefore, the NN output will be a pair of parameters from the Beta distribution (α and β) for each action. For this stochastic beta policy, only the cases where $\alpha, \beta > 1$ were considered, since solely in this domain the distribution is concave and unimodal.

During the training stage, actions are sampled from the probability density function (PDF)(Eq. 3) in order to provide exploration, while during evaluation the stochasticity is removed and actions are selected as the mean of the PDF (Eq. 6).

$$Beta_{PDF} = \frac{x^{\alpha-1}(1-x)^{\beta-1}}{B(\alpha, \beta)} \quad (3)$$

$$B(\alpha, \beta) = \frac{\Gamma(\alpha)\Gamma(\beta)}{\Gamma(\alpha + \beta)} \quad (4)$$

$$\Gamma(z) = \int_0^\infty x^{z-1} e^{-x} dx \quad (5)$$

$$Beta_{mean} = \frac{\alpha}{\alpha + \beta} \quad (6)$$

The complete configuration of the PPO agent is provided in Appendix A.

5.2.2. Environment

The environment of the pumping station is described in section 5.1.

5.2.3. State

The state representation is a combination of the current snapshot of the environment and the WWIR forecasts presented in section 4, namely:

- Current tank level
- Pumps online (excluding units in maintenance or offline), which is a binary vector with the pump status
- Current WWIR
- Current set point for each individual pump
- Probabilistic forecasts of WWIR: 25%, 50% and 75% quantiles for 20 steps ahead

5.2.4. Actions

The actions sampled from the control policy are the power set-points for each individual pump unit.

5.2.5. Reward

The reward function quantifies the performance of the control policy, acting as the only feedback that allows the control policy to learn the correct action for a given state.

Equation 7 defines the reward function used in this problem. As observed, the reward is divided into two terms: i) tank level and ii) power consumption. $c1$ and $c2$ are constants which give relative weight to each one of the terms, and are ordered according to the objective of the problem. Since it is more important to avoid overflow of the tank than to decrease the energy consumption: $c1 > c2$. The following sub-sections detail both parcels of the reward function.

$$r_t = c1 \cdot r_{WWlevel_t} + c2 \cdot r_{power_t} \quad (7)$$

It is important to stress that the values $c1$ and $c2$ should be defined by the end-user according to its requirements. A sensitive analysis of these parameters is provided in section 6.3.

Wastewater Reservoir Level, $r_{WWlevel_t}$

The first term rewards the policy for operating with the tank level within the admissible limits. If the level is between 3m and 7.2m, a reward of R^+ is given, otherwise a reward of R^- is issued. An empirical analysis showed good results with $R^+ = 3$ and $R^- = -600$. It is relevant to stress that it is important to have a much severe penalty than a reward, since the first objective is to operate within the tank limits. Mathematically it is translated into:

$$r_{WWlevel,t} = \begin{cases} R^+, & h \in [3.0, 7.2] \\ R^-, & h \in [0, 3.0[\vee h \in]7.2, 8.0] \end{cases} \quad (8)$$

Power Consumption, r_{power_t}

Since the control strategy aims to decrease the power consumption of the WWPS, for each timestep t a penalty proportional to the total installed capacity of the pumping

station is applied as follows:

$$r_{power_t} = \frac{\sum_i P_{i,t}}{P_{inst}} \quad (9)$$

where $P_{i,t}$ is the power consumption of the i -th pump for timestep t and P_{inst} the total capacity of the pumping station.

5.2.6. RL Agent Learning Process

The training process consists on performing a set of actions for several iterations, using the simulated environment and two sets of episodes: one for training and the other to continuously assess the performance of the control policy.

The policy NN is initialized by assigning random values to its weights and bias. Then an iterative learning process takes place until the predefined number of iterations is reached. Each iteration is divided into two phases: training and test.

The training process consists on randomly select an episode and allowing the RL agent to interact with the simulated environment for T timesteps. In this stage, both the policy and the environment are stochastic in order to provide exploration. Since the policy is represented by a beta distribution, the actions are obtained taking samples from the PDF. In the environment, the stochasticity is provided by randomizing the water level in the tank at the start of each episode. In each interaction (step) the control policy receives as input the state of system (as described in Section 5.2.3) and chooses an action representing the operational set-point for each one of the pumps. The action is applied to the environment which leads the system to a new state and the emission of a reward. For each step the state transition vector (observation, action, reward) is collected, and this episodic rollout ends at the terminal stage of an episode (either by reaching the maximum number of steps or by getting an alarm). Afterwards, the collected vector is used to train the RL agent using the PPO algorithm, altering the policy parameters (weights and bias of the neural network).

The recently updated policy is then used in the second stage, and is used to assess its performance in a small subset of the available testing episodes. In this stage the stochasticity is removed to allow reproducibility between iterations, thus leading to a fairer comparison and analysis. The statistics collected during this stage (average reward,

number of alarms and energy consumption) are used to evaluate the learning process. This concludes an iteration of the learning process and the policy restarts the collection of the transitions vector.

6. Numerical Results

The energy optimization strategy was applied to the WWPS described in section 2.

Using the historical records collected by the station’s SCADA system, a set of episodes were created for evaluating the control performance, i.e. 80% were chosen to train the RL agent while the remaining 20% were used as the test set. Due to some missing values in the original dataset, the episodes have variable length in order to maximize the amount of continuous steps.

A minimum of 200 timesteps was enforced per episode, while the maximum was left uncapped, leading to some episodes with more than 3000 timesteps. Each episode contains information about the number of online pumping units (excluding the ones in maintenance or unavailable), current WWIR and WWIR forecasts. This information is discretized in 2-minute steps.

The numerical results presented below were obtained by applying the RL agent to all the episodes of the testing set, which comprises 65 episodes, encompassing more than 64,000 steps for a total of 90 days of data.

Four scenarios were considered to measure the performance of the data-driven optimization strategy:

- Current operating rules
- Strategy without WWIR forecasts
- Strategy with WWIR forecasts
- Strategy with perfect WWIR forecasts (i.e. observed values)

The first scenario is used as the benchmark model since it corresponds to the historical records of the current operation of the WWPS. The other three scenarios aim to assess the improvement of the RL agent in comparison with current control operation and also to compare the predictive aspect of RL agent by evaluating an agent with access

to WWIR forecasts. The perfect forecast scenario establishes an upper bound for the electrical energy saving gains.

The following sections show a set of numerical analysis considering these four scenarios. It is important to underline that the RL learning process has an inherent instability. As mentioned before, for each learning iteration the control policy is applied to the test set and the relevant performance indicators are collected. Furthermore, instead of considering the best iteration of all the learning process, it is considered the last 5000 iterations to smooth the variability. The results are presented as a set of quantiles (25%, 50% and 75%) to better illustrate the variability in performance from iteration to iteration.

6.1. Improvement in the Number of Alarms

The WWPS has preventive measures to avoid spillage of wastewater during periods of extreme WWIR. There are two critical alarm levels, the first at 7.2 meters initiates a preventive action that re-directs a share of the incoming wastewater directly to the output of the facility and skipping some treatment phases. The second alarm occurs at the 8 meters when the tank reaches its maximum capacity and overflow occurs.

This section studies the number of alarms triggered in the four scenarios under evaluation. Results are depicted in Figure 15 and Table 2.

Figure 15 shows the number of alarms registered when operating the WWPS using the RL control for the past 5000 iterations of the training process. The depicted dots represent the number of alarms while the shaded area indicates the 25% and 75% quantiles of the same record. The top plot shows the control results without WWIR forecasts in the state vector, the middle plot shows the predictive control with probabilistic WWIR forecasts, and the bottom one indicates the alarm performance considering perfect information of WWIR. Without WWIR forecasts the number of alarms ranges from 4 to 11, while with the predictive control the number of alarms is kept between 4 and 6, and, as seen in the plot, with much less variability. With perfect forecast (or knowledge) for the WWIR, the predictive control maintains an alarm number of 4. As will be discussed later, 4 alarms are the minimum possible number, since these alarms occurred at the start of the episode, therefore unavoidable for the RL control strategy.

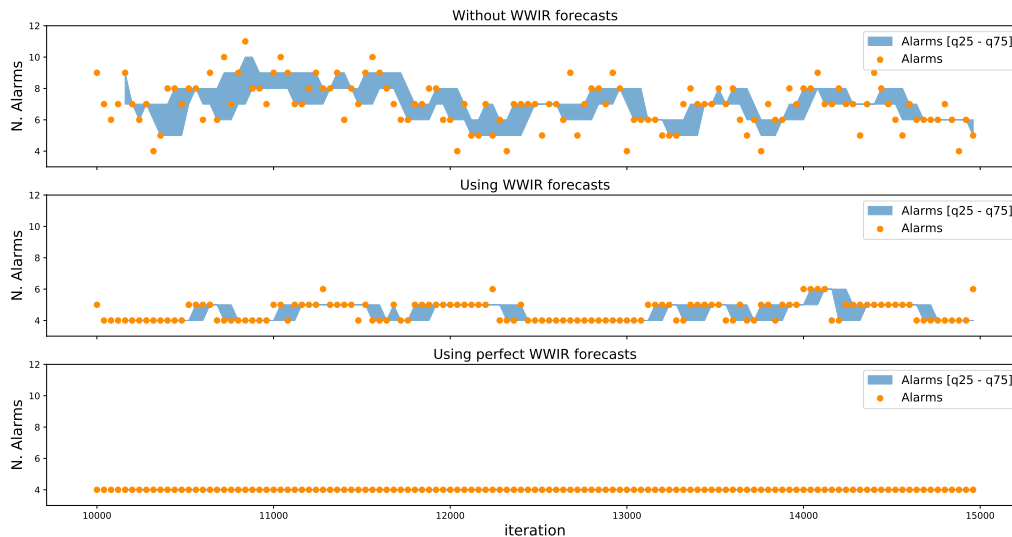


Figure 15: Number of alarms (wastewater level above 7.2m) with and without WWIR forecasts.

Table 2 shows a comparison between the RL control strategy and the current operational procedure. Considering the episodes under evaluation, a total of 1671 occurrences were originally registered of wastewater level above the first alarm trigger (7.2 meters). Despite the previous numbers, the second alarm was never triggered, registering a maximum level of 7.98 meters.

The RL approach was able to significantly reduce the number of alarms triggered, for both the predictive and non-predictive strategies. Without WWIR forecasts, the RL strategy registered an average of 7 alarms, and by including the probabilistic forecasts this number decreased to 4.55 alarms in average, for the last 5000 training iterations.

Table 2: Number of reservoir level alarms triggered.

	Alarms 7.2m			Alarms 8m
	q25%	q50%	q75%	n. occur
Current operating rules		1671		0
RL without WWIR forecasts	6.47	7.05	7.54	0
RL with WWIR forecasts	4.36	4.55	4.68	0
RL with perfect WWIR forecasts	4.0	4.0	4.0	0

Providing a set of probabilistic forecasts to the RL agent adds the possibility to anticipate changes in the WWIR and adjust the pumping operation accordingly. Figure 16 illustrates this capability. The top plot depicts the tank level for the scenarios of current operating rules and RL agent with WWIR forecasts; the bottom plot shows the observed WWIR. The control strategy operates at a tank level close to the first alarm trigger in order to optimize the electrical energy consumption, but when the forecasts show an expected increasing rate of WWIR the pumping activity is increased to provide a sufficient buffer to accommodate the expected increase of the tank level. In the current operating rules scenario, the control strategy is not quick enough to adapt to the changing rates and the first alarm is triggered during some time period.

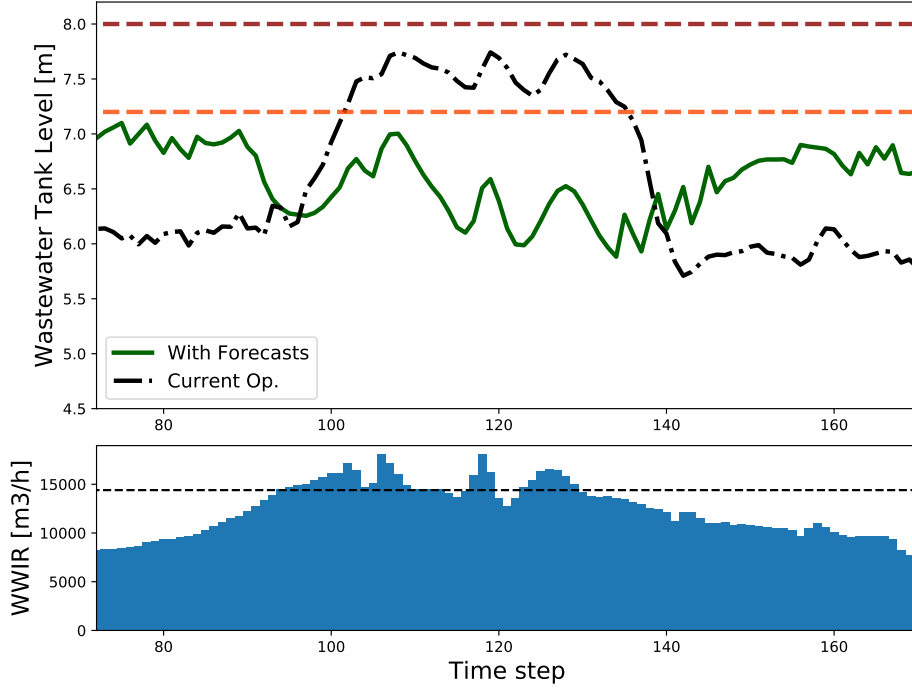


Figure 16: Predictive control avoiding an alarm.

Despite the significant improvement in performance of the RL control strategy, in comparison with the benchmark operation, it still registers a few alarms. However, some of these alarms occurred in unavoidable situations. After dividing the historical dataset into segments, some of the episodes start with the tank level already above the first

alarm. In fact, four of the registered alarms occurred in the first and second steps of an episode, which are unavoidable for the control strategy (even with perfect WWIR forecasts). Figure 17 depicts one of those situations where the starting tank level was already above the alarm trigger and therefore unavoidable. However, the RL agent was able to significantly reduce the amount of timesteps with tank above 7.2 meters.

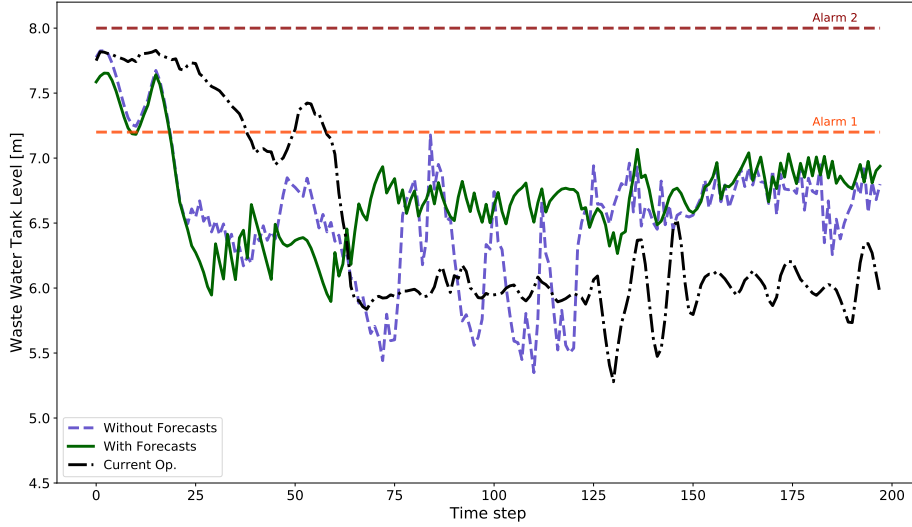


Figure 17: Alarm triggered due to an episode start.

6.2. Improvement in Electrical Energy Consumption

This section studies the ability of the proposed control strategy to reduce the electrical energy consumption of the WWPS process. Following the methodology presented in the previous section, Figure 18 depicts the comparison between the predictive and non-predictive RL control, while Table 19 shows the results for the absolute values of electrical energy consumption for the four scenarios under evaluation plus the improvement of the RL control in comparison with the current operating rules.

The results in Figure 18 show that the non-predictive control registered a cumulative energy consumption ranging between 459 MWh and 469 MWh, while the predictive control was able to operate with significantly less electrical energy needs, obtaining values between 362 MWh and 379 MWh. The scenario with WWIR perfect forecasts showed an electrical energy consumption between 340 MWh and 348 MWh.

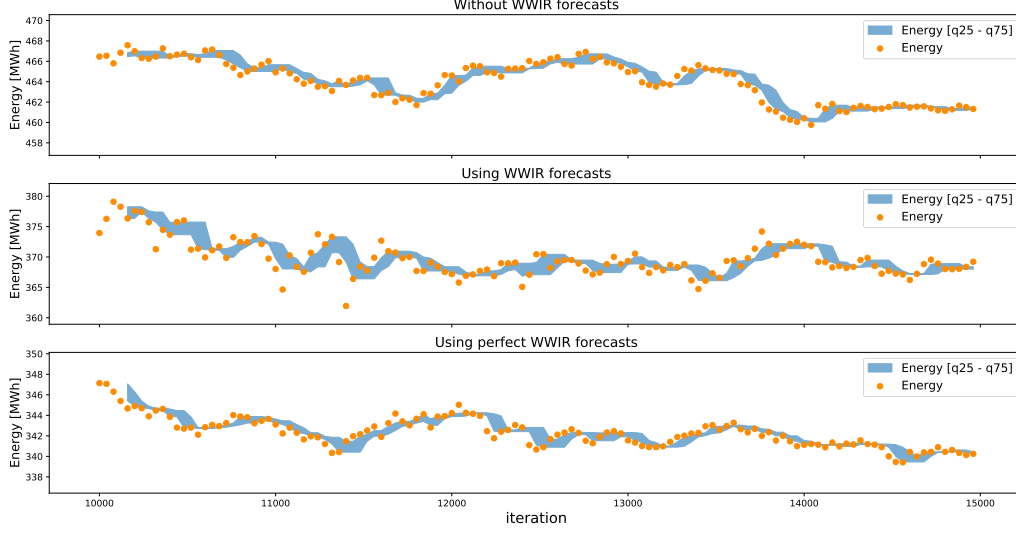


Figure 18: Electrical energy consumption with and without WWIR forecasts.

From Table 3 it is possible to observe that the current operating rules required a cumulative electrical energy consumption of 379.8 MWh. In comparison, the non-predictive strategy required more 22% than the current operation, while using WWIR probabilistic forecasts as input resulted in an added value since the electrical energy needs reduced by almost 3%. It is important to underline that with perfect WWIR forecasts, the control strategy was able to achieve an improvement of 9.95%.

Table 3: Electrical energy consumption in the three scenarios: current operating rules, with and without WWIR forecasts.

	Energy Consumption [MWh]			Improvement q50%
	q25%	q50%	q75%	
Current operating rules	379.8			—
RL without WWIR forecasts	463.7	464.0	464.3	-22.19%
RL with WWIR forecasts	369.0	369.7	370.5	2.66%
RL with perfect WWIR forecasts	342.0	342.32	342.57	9.95%

The amount of energy consumption required to operate the WWPS has a direct relation with the average wastewater tank level, i.e. a higher level requires less power to

pump the same amount of wastewater. Table 4 shows the average and standard deviation of wastewater tank level for the four scenarios under evaluation. As expected, with the WWIR forecast for the 20-steps ahead, the control strategy is able to operate the facility at almost more 30 centimeters higher than the current operation, justifying the electrical energy savings. Furthermore, the scenario with perfect WWIR forecasts obtained an average tank level of 6.58 m.

Table 4: Wastewater tank level in the three scenarios: current operating rules, with and without WWIR forecasts.

	Wastewater level	
	mean [m]	std [m]
Current operating rules	6.05	0.39
RL without WWIR forecasts	6.06	0.35
RL with WWIR forecasts	6.36	0.21
RL with perfect WWIR forecasts	6.58	0.15

Figure 19 depicts an episode where it is possible to observe the lower electrical energy needs of the RL strategy in comparison to the current operating rules. The top plot shows the tank level while the bottom plot the cumulative electrical energy consumption. In the current operation scenario, the pumps are operated in order to keep the tank level around 6 meters, while the RL strategies are free to choose the optimal operation point. As a result, the strategy which uses WWIR forecasts is able to operate very close to the first alarm trigger in order to reduce the electrical energy use. The use of the forecasts provides the strategy with a snapshot of the following moments and allows operating closer to the alarm while maintaining the risk under control.

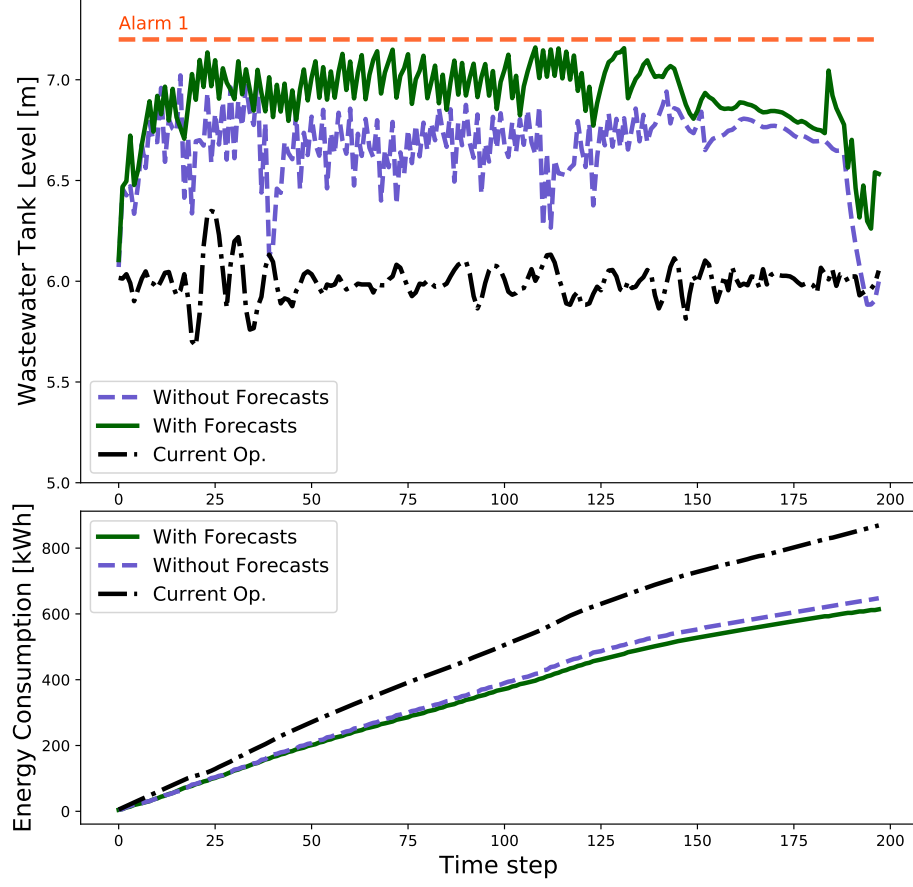


Figure 19: Wastewater level and energy consumption in the three scenarios: current operating rules, with and without WWIR forecasts.

6.3. Trade-off Between Alarms and Electrical Energy Consumption

As discussed in Section 5.2.5, in the reward function the coefficients $c1$ and $c2$ represent the weight assigned to both objectives of the control strategy: alarms and electrical energy consumption reduction, respectively. In this section, the impact of changing these values is analyzed.

Two scenarios were considered:

- **Scenario^{alarms}**: prioritizes the reduction on the number of alarms ($c1 = 1$; $c2 = 0.5$) and

- **Scenario^{energy}** emphasizes the electrical energy consumption reduction ($c1 = 0.5$; $c2 = 1$)

Figure 20 presents a comparison between the two scenarios. The top plot depicts the number of alarms and the energy consumption is presented in the bottom plot. In Scenario^{alarms}, the number of alarms is low, ranging between 4 and 7, while the other scenario reaches numbers between 29 and 48. By analyzing the electrical energy consumption, it is possible to detect a considerable difference between both scenarios, i.e. Scenario^{alarms} has a energy consumption ranging from 366 MWh to 377 MWh, while Scenario^{energy} shows between 315 MWh and 318 MWh.

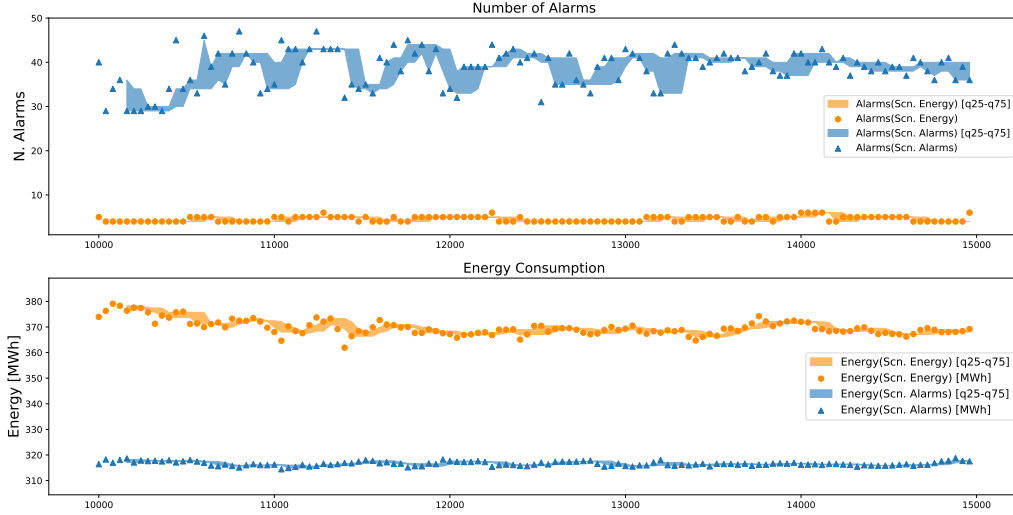


Figure 20: Number of alarms versus electrical energy consumption in the two scenarios

Table 5 details the average values for alarms and electrical energy consumption for both scenarios and the current operating control rules, plus the improvement obtained with the RL control. As seen in Figure 20, Scenario^{energy} obtains a lower energy consumption at the cost of more alarms. To put this increase in perspective, even with the record of more than 38 alarms, the Scenario^{energy} lead to a decrease of almost 98% in the number of alarms when compared with the current operation. On the other hand, the energy consumption decreases almost 17% when compared with the current operating rules, while with the Scenario^{alarms} the decrease was only 2.66%. Therefore, these results show that with the proposed methodology, significant reduction in electrical energy con-

sumption can be obtained with a minor increase in the number of alarms. In all cases, the improvement in both criteria was obtained compared to the current operating rules.

Table 5: Comparison between the current operating rules and the two scenarios under evaluation: Scenario^{alarms} and Scenario^{energy}.

	Energy [MWh]	Alarms	Improvement	
			Energy	Alarms
Scenario ^{alarms}	369.7	4.55	2.66%	99.73%
Scenario ^{energy}	316.5	38.7	16.67%	97.68%
Current operating rules	379.8	1671	—	—

7. Conclusions

The present work proposes a data-driven optimization framework for the operation of a wastewater pumping station. This work explores machine learning techniques that produce probabilistic forecasts for the wastewater intake rate and construct a data-driven proxy for the physical system. By feeding a reinforcement learning algorithm with these forecasts and proxy models, a predictive control algorithm is implemented to optimize (i.e. minimize electrical energy consumption and alarms for tank level above limit) the operation of wastewater pumps by actuating in its active power set-points.

Operating the wastewater pumping station optimally depends on the trade-off between the number of alarms (tank level above 7.2 meters) and the electrical energy consumption of the facility. The results in a real-world wastewater pumping station for 90 non-consecutive days showed an higher performance both in terms of energy efficiency and alarms. If priority is given to the operation within the wastewater tank limits, the proposed control strategy was able to nearly mitigate them, obtaining just 4 alarms that occurred in unavoidable situations (99% less than the current operating rules). Furthermore, a decrease of almost 3% of the overall electrical energy needs of the pumping station was also verified. On the other hand, if more weight is given to the electrical energy component, the control strategy registered 39 alarms (still meaning a 97% decrease in comparison with the current procedures) while improving the energy efficiency in 17%.

Finally, it is important to mention that around 20% of the operational costs in the company's WWTP were associated to the wastewater pumping stations. Therefore, the benefits of the proposed method could be translated into a significant reduction of the global energy consumption.

Acknowledgements

The research leading to this work is being carried out as a part of the InteGrid project (*Demonstration of INTElligent grid technologies for renewables INTEgration and INTER-active consumer participation enabling INTERoperable market solutions and INTERconnected stakeholders*), which received funding from the European Union's Horizon 2020 Framework Programme for Research and Innovation under grant agreement No. 731218.

The sole responsibility for the content lies with the authors. It does not necessarily reflect the opinion of the Innovation and Networks Executive Agency (INEA) or the European Commission (EC). INEA or the EC are not responsible for any use that may be made of the information it contains.

Appendix A. PPO Configuration

Table A.6: Proximal policy optimization configuration

variable	value
Num iterations	15k
Policy layers	[64, 64]
Value Function layers	[64, 64]
Activation function	ReLU
Timesteps per update	750
Batch size	250
Learning rate	1.5e-4 (decaying exponentially)
Entropy loss	0.0
Clip param.	0.2
γ	0.99
δ	0.95
Reward scale	600
Reward: R^+	3
Reward: R^-	-600
Reward: c_1	1
Reward: c_2	0.4

References

References

- [1] Managing Water for All: An OECD Perspective on Pricing and Financing, Technical Report, OECD, 2009.
- [2] A. Guerrini, G. Romano, C. Leardini, M. Martini, Measuring the efficiency of wastewater services through data envelopment analysis, *Water Science and Technology* 71 (2015) 1845–1851.
- [3] A. Rasekh, A. Hassanzadeh, S. Mulchandani, S. Modi, M. K. Banks, Smart water networks and cyber security, *Journal of Water Resources Planning and Management* 142 (2016) 1–3.
- [4] A. S. Wayal, S. V. Deshmukh, Energy audit of water and wastewater treatment plants. a review, in: 49th Annual Convention of Indian Water Works Association (IWWA) on Smart Water Management, Nagpur, India.

- [5] F. O. Kebir, M. Demirci, M. Karaaslan, E. Ünal, F. Dincer, H. T. Aratç, Smart grid on energy efficiency application for wastewater treatment, *Environmental Progress & Sustainable Energy* 33 (2014) 556–563.
- [6] A. S. V. Kalaiselvan, U. Subramaniam, P. Shanmugam, N. Hanigovszki, A comprehensive review on energy efficiency enhancement initiatives in centrifugal pumping system, *Applied Energy* 181 (2016) 495–513.
- [7] L. M. Brion, L. W. Mays, Methodology for optimal operation of pumping stations in water distribution systems, *Journal of Hydraulic Engineering* 117 (1991) 1551–1569.
- [8] P. W. Jowitt, G. Germanopoulos, Optimal pump scheduling in water-supply networks, *Journal of Water Resources Planning and Management* 118 (1992) 406–422.
- [9] R. Menke, E. Abraham, P. Parpas, I. Stoianov, Exploring optimal pump scheduling in water distribution networks with branch and bound methods, *Water Resources Management* 30 (2016) 5333–5349.
- [10] M. López-Ibáñez, T. D. Prasad, B. Paechter, Optimal pump scheduling: Representation and multiple objectives, in: *Proceedings of the eighth International Conference on Computing and Control for the Water Industry*, volume 1, pp. 117–122.
- [11] R. Kernan, X. Liu, S. McLoone, B. Fox, Demand side management of an urban water supply using wholesale electricity price, *Applied Energy* 189 (2017) 395–402.
- [12] A. Jacobusvan, J. Zhang, X. Xia, A model predictive control strategy for load shifting in a water pumping scheme with maximum demand charges, *Applied Energy* 88 (2011) 4785–4794.
- [13] P. Palensky, D. Dietrich, Demand side management: Demand response, intelligent energy systems, and smart loads, *IEEE Transactions on Industrial Informatics* 7 (2011) 381–388.
- [14] G. Bonvin, S. Demasse, C. L. Pape, N. Maïzi, V. Mazauric, A. Samperio, A convex mathematical program for pump scheduling in a class of branched water networks, *Applied Energy* 185 (2017) 1702–1711.
- [15] X. Zhuan, X. Xia, Optimal operation scheduling of a pumping station with multiple pumps, *Applied Energy* 104 (2013) 250–257.
- [16] R. Menke, E. Abraham, P. Parpas, I. Stoianov, Demonstrating demand response from water distribution system through pump scheduling, *Applied Energy* 170 (2016) 377–387.
- [17] P. J. Nybo, C. S. Kallesøe, K. G. Lauridsen, Method for operating a wastewater pumping station, 2014. U.S. Patent Application No. 14/133,938.
- [18] M. Fiter, D. Güell, J. Comas, J. Colprim, M. Poch, I. Rodríguez-Roda, Energy saving in a wastewater treatment process: an application of fuzzy logic control, *Environmental Technology* 26 (2005) 1263–70.
- [19] S. Syafie, F. Tadeo, E. Martinez, T. Alvarez, Model-free control based on reinforcement learning for a wastewater treatment problem, *Applied Soft Computing* 11 (2011) 73–82.
- [20] F. H. del Olmo, E. Gaudioso, A. Nevado, Autonomous adaptive and active tuning up of the dissolved oxygen setpoint in a wastewater treatment plant using reinforcement learning, *IEEE Transactions on Systems, Man, and Cybernetics, Part C (Applications and Reviews)* 42 (2012) 768–774.

- [21] A. Asadi, A. Verma, K. Yang, Wastewater treatment aeration process optimization: A data mining approach, *Journal of Environmental Management* In Press (2016).
- [22] X. Wei, A. Kusiak, Short-term prediction of influent flow in wastewater treatment plant, *Stochastic Environmental Research and Risk Assessment* 29 (2015) 241–249.
- [23] Z. Zhang, A. Kusiak, Models for optimization of energy consumption of pumps in a wastewater processing plant, *Journal of Energy Engineering* 137 (2011) 159–168.
- [24] Z. Zhang, Y. Zeng, A. Kusiak, Minimizing pump energy in a wastewater processing plant, *Energy* 47 (2012) 505–514.
- [25] Y. Zeng, Z. Zhang, A. Kusiak, F. Tang, X. Wei, Optimizing wastewater pumping system with data-driven models and a greedy electromagnetism-like algorithm, *Stochastic Environmental Research and Risk Assessment* 30 (2016) 1263–1275.
- [26] Z. Zhang, A. Kusiak, Y. Zeng, X. Wei, Modeling and optimization of a wastewater pumping system with data-mining methods, *Applied Energy* 164 (2016) 303–311.
- [27] Z. Zhang, X. He, A. Kusiak, Data-driven minimization of pump operating and maintenance cost, *Engineering Applications of Artificial Intelligence* 40 (2015) 37–46.
- [28] C. K. Yoo, D. S. Kim, J.-H. Cho, S. W. Choi, I.-B. Lee, Process system engineering in wastewater treatment process, *Korean Journal of Chemical Engineering* 18 (2001) 408–421.
- [29] R. Koenker, G. Bassett, Regression quantiles, *Econometrica* 46 (1978) 33–50.
- [30] S. Seabold, J. Perktold, Statsmodels: Econometric and statistical modeling with python, in: *Proceedings of the 9th Python in Science Conference*, volume 57.
- [31] J. H. Friedman, Greedy function approximation: A gradient boosting machine, *Annals of Statistics* 29 (2001) 1189–1232.
- [32] F. Pedregosa, G. Varoquaux, A. Gramfort, V. Michel, B. Thirion, O. Grisel, M. Blondel, P. Prettenhofer, R. Weiss, V. Dubourg, J. Vanderplas, A. Passos, D. Cournapeau, M. Brucher, M. Perrot, E. Duchesnay, Scikit-learn: Machine learning in python, *Journal of Machine Learning Research* 12 (2011) 2825–2830.
- [33] P. Pinson, H. A. Nielsen, J. K. Møller, H. Madsen, G. N. Kariniotakis, Non-parametric probabilistic forecasts of wind power: required properties and evaluation, *Wind Energy* 10 (2007) 497–516.
- [34] S. B. Taieb, R. Huser, R. J. Hyndman, M. G. Genton, Forecasting uncertainty in electricity smart meter data by boosting additive quantile regression, *IEEE Transactions on Smart Grid* 7 (2016) 2448–2455.
- [35] J. Snoek, H. Larochelle, R. P. Adams, Practical bayesian optimization of machine learning algorithms, in: *Advances in Neural Information Processing Systems* 25 (NIPS 2012), pp. 2951–2959.
- [36] J. Schulman, F. Wolski, P. Dhariwal, A. Radford, O. Klimov, Proximal policy optimization algorithms, *arXiv:1707.06347 abs/1707.06347* (2017).
- [37] J. Schulman, P. Moritz, S. Levine, M. I. Jordan, P. Abbeel, High-dimensional continuous control using generalized advantage estimation, *CoRR* abs/1506.02438 (2015).